

Elemental Chalcogen Activation | *Very Important Paper* |

## VIP Activation of Elemental Sulfur at a Two-Coordinate Platinum(0) Center

Sudipta Roy,<sup>[a, b]</sup> Christian J. Schürmann,<sup>[a]</sup> Totan Mondal,<sup>[c]</sup> Debasis Koley,<sup>\*[c]</sup> Regine Herbst-Irmer,<sup>[a]</sup> Dietmar Stalke,<sup>\*[a]</sup> and Herbert W. Roesky<sup>\*[a]</sup>

**Abstract:** Platinum dichalcogenides have been known to exhibit two-dimensional layered structures. Herein, we describe the syntheses, isolation, and characterization of air-stable crystalline cyclic alkyl(amino) carbene (cAAC)-supported monomeric platinum disulfide three-membered ring complex [(cAAC)<sub>2</sub>Pt(S<sub>2</sub>)] (**2**). The highly reactive platinum(0) [(cAAC)<sub>2</sub>Pt] complex (**1**) with two-coordinate platinum activates elemental sulfur to give **2**. The brown crystals of bis-carbene platinum(II)monosulfate [(cAAC)<sub>2</sub>Pt(SO<sub>4</sub>)<sub>x</sub>(S<sub>2</sub>)<sub>1-x</sub>] (**4**) have been isolated when the reaction was performed in air. The dioxygen analogue of **2** was formed upon exposing the THF solution of **1** to aerial oxygen (O<sub>2</sub>). The binding of oxygen at the Pt<sup>0</sup> center was found to be reversible. Additionally, DFT study has been performed to elucidate the electronic structure and bonding scenario of **2**, **3**, and **4**. Quantum chemical calculations showed donor-acceptor-type interaction for the Pt-S bonds in **2** and Pt-O bonds in **3** and **4**.

Platinum disulfide (PtS<sub>2</sub>) has been first synthesized by Davey in 1814 by treating hexachloroplatinate(IV) with sulfur at very high temperatures in the absence of air.<sup>[1]</sup> The structural characterization of crystalline PtS<sub>2</sub> was reported by Grønvold and Kjekshus, which revealed a two-dimensional layered structure of the type CdI<sub>2</sub>.<sup>[2]</sup> In 1970, PtS<sub>2</sub> has been concluded to have a suitable band gap, which is required to display semiconduct-

ing properties.<sup>[3]</sup> Moreover, sulfur-containing metal complexes are very important in various biological reactions and in petroleum-refining processes.<sup>[4]</sup> Platinum can attain a broad range of oxidation states from -3 to +10: it can exhibit a very rich redox chemistry.<sup>[5-7]</sup> However, the excellent bridging ability of sulfur often leads to the formation of polynuclear sulfur-bridged metal complexes.<sup>[8]</sup> In this context, it is worthy to mention that strong  $\sigma$ -donating ligands can be effectively utilized to hinder the vacant coordination sites of metals from receiving further donations. This prevents metal-sulfur complexes from undergoing aggregation.<sup>[9]</sup> Since the first report on cyclic alkyl(amino) carbenes (cAACs),<sup>[10]</sup> it has been often stated that they are the more advantageous ligands for the stabilization of various reactive species compared to NHCs.<sup>[11]</sup> Group 10 metal complexes with low-coordinate metals and oxidation state zero have attracted enormous attention of the synthetic chemists due to their proposed function as intermediates in various organometallic reaction protocols. Very recently, the syntheses, isolation, and characterization of cAAC-stabilized complexes of nickel(0), palladium(0), and platinum(0) with two-coordinate metal atoms were reported.<sup>[12]</sup> cAAC is a stronger  $\sigma$  donor and even a better  $\pi$  acceptor. Moreover, cAAC can keep the balance between its  $\sigma$  donation and  $\pi$  acceptance properties to be in tune with the electronic requirements necessary for small-molecule activation. To date, only the activation of molecular hydrogen by these highly reactive (carbene)<sub>2</sub>M complexes with low-coordinate metals has been reported [M = Mn].<sup>[13a]</sup> The activation of chalcogens by (carbene)<sub>2</sub>M<sup>0</sup> complexes has been not known to date. Monomeric side-on MS<sub>2</sub> complexes of transition metals have been known for almost five decades [M = Nb, Ir, Rh].<sup>[13b-d]</sup> Oxidation of MS<sub>2</sub> complexes to give the corresponding oxidized complexes of the sulfur oxides S<sub>2</sub>O and S<sub>2</sub>O<sub>2</sub> are known.<sup>[13e-g]</sup> However, Pt analogues are not reported until now. Herein, we report the syntheses, isolation, and characterization of the cAAC-stabilized monomeric platinum(II)disulfide [(cAAC)<sub>2</sub>Pt(S<sub>2</sub>)] (**2**; Scheme 1) and the partially oxidized product platinum sulfate [(cAAC)<sub>2</sub>Pt(SO<sub>4</sub>)<sub>x</sub>(S<sub>2</sub>)<sub>1-x</sub>] (**4**). Complex (cAAC)<sub>2</sub>Pt (**1**) also reacted with aerial oxygen to form complex (cAAC)<sub>2</sub>PtO<sub>2</sub> (**3**; Scheme 1). The bonding and electronic distributions of complexes **2**, **3**, and **4** were studied by theoretical calculations (for computational details, see the Supporting Information).

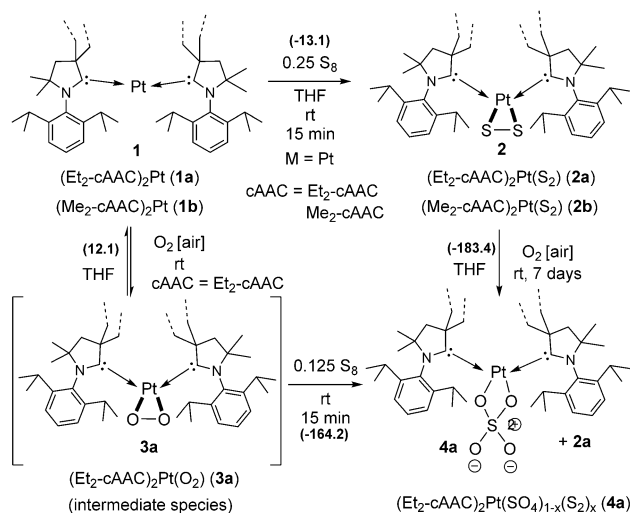
The precursor complex (cAAC)<sub>2</sub>Pt (**1**) [(Et<sub>2</sub>-cAAC)<sub>2</sub>Pt, **1a**; (Me<sub>2</sub>-cAAC)<sub>2</sub>Pt, **1b**]<sup>[14]</sup> was dissolved in THF and the resultant orange solution was transferred into a flask containing 0.25 equivalents of S<sub>8</sub> at room temperature with continuous

[a] Dr. S. Roy, C. J. Schürmann, Dr. R. Herbst-Irmer, Prof. Dr. D. Stalke, Prof. Dr. H. W. Roesky  
Institut für Anorganische Chemie, Georg-August-Universität  
Tammannstrasse 4, 37077 Göttingen (Germany)  
Fax: (+49) 551 39 3373  
E-mail: dstalke@chemie.uni-goettingen.de  
hroesky@gwdg.de

[b] Dr. S. Roy  
Department of Chemistry  
Indian Institute of Science Education and Research (IISER) Tirupati  
Karakambadi Road 517507, Tirupati, Andhra Pradesh (India)

[c] T. Mondal, Dr. D. Koley  
Department of Chemical Sciences  
Indian Institute of Science Education and Research (IISER) Kolkata  
Mohanpur 741246 (India)  
E-mail: koley@iiserkol.ac.in

Supporting information for this article can be found under  
<http://dx.doi.org/10.1002/chem.201603030>. It contains the syntheses and characterizations of complexes **1-4**, as well as crystal-structure determination of **1-THF**, **1-3-0.5 THF**, **4-THF**, **5-0.5 THF**, and **6-0.5 THF**.



**Scheme 1.** Syntheses of complexes 2–4 from 1. The energy term in parenthesis is  $\Delta G_{298}^\ddagger$  [kcal mol<sup>-1</sup>] at the M06/def2-TZVP/SMD//M06/def2-SVP level of theory for 2a to 4a.

stirring. After 15 minutes, the color of the reaction solution changed to red, and then slowly faded to a light purple after 30 minutes upon vigorous stirring. The reaction solution was then concentrated and stored at  $-32^\circ\text{C}$  in a freezer to form purple crystals of complex 2 in 70–74% yield. The crystals of 2 are stable in air for several days at room temperature. The solution of 2 is also stable in air for 3–4 days, and then it is partially oxidized to 4. Powders of 2a and 2b melt above 175 and 218  $^\circ\text{C}$ , respectively. The THF solutions of 2a and 2b are stable at  $-32^\circ\text{C}$  to room temperature for several months under inert atmosphere. Compound 2a is soluble in polar solvents, for example, THF, whereas 2b is highly crystalline and only sparingly soluble. The  $^{13}\text{C}$  NMR spectrum of 2a in  $[\text{D}_8]\text{THF}$  solution exhibited a resonance at  $\delta = 256.44$  ppm for  $\text{C}_{\text{CAAC}}$ , flanked by a pair of  $^{195}\text{Pt}$  satellites ( $J_{\text{Pt-C}} = 1396.7$  Hz), which is slightly upfield shifted compared with that of the precursor 1 (258.76 ppm,  $J_{\text{Pt-C}} = 1150.7$  Hz). The  $^{195}\text{Pt}$  NMR spectrum of 2a showed a singlet at  $\delta = -4308.47$  ppm, which is also downfield shifted compared with that of the precursor 1 at  $-4333.82$  ppm. The UV/Vis spectrum of 2a was recorded in THF, which showed a broad absorption band at  $\lambda = 575$  nm (see the Supporting Information), which is close to the theoretically computed value at  $584\text{ cm}^{-1}$  (TD-M06/def2-TZVP level of theory). The  $\tilde{\nu}_{\text{S-S}}$  vibration of 2a was observed at  $515\text{ cm}^{-1}$  (see the Supporting Information), which is close to the theoretically computed value at  $539\text{ cm}^{-1}$  (M06/def2-SVP level of theory). Complexes 2a and 2b were further characterized by electron ionization mass spectrometry (ESI-MS) in MeCN ( $[\text{M}+\text{H}]^+$   $m/z$ : 2a: 886.4669; 2b: 830.4033; see the Supporting Information).

When the lighter analogues  $(\text{cAAC})_2\text{Ni}^0$  and  $(\text{cAAC})_2\text{Pd}^0$  were treated with sulfur under similar reaction condition,  $\text{cAAC}=\text{S}$  was isolated (see the Supporting Information).

When a 4:1 mixture of complex 1a and  $\text{S}_8$  were reacted under air in THF, a dark red-brown colored solution was obtained after 30 minutes of stirring. The concentrated THF solution was stored at room temperature for one week to obtain

air-stable purple crystals of 4a in 10% yield. Synthesis of 4a was assumed to proceed via the initial formation of the intermediate species  $[(\text{cAAC})_2\text{PtO}_2]$  (3a) from 1a by activation of molecular oxygen at the  $\text{Pt}^0$  atom of 1. This could be attributed by the color change of the THF solution of 1a from bright orange to dark red when the solution was kept under air for a day. The UV/Vis spectrum of this dark red solution was recorded and displays strong absorption bands at  $\lambda = 212, 281, 316, 360$  and  $450$  nm. The in situ formation of the intermediate species  $[(\text{cAAC})_2\text{PtO}_2]$  (3a) was further investigated by NMR spectroscopy and confirmed by mass spectrometry (see the Supporting Information). The  $^{13}\text{C}$  NMR spectrum of 3a recorded in  $[\text{D}_8]\text{THF}$  exhibits a singlet at  $\delta = 249.52$  ppm for the  $\text{C}_{\text{carbene}}$  which was upfield shifted compared with that of the precursor 1a ( $\delta = 258.0$  ppm). The  $^{195}\text{Pt}$  NMR spectrum of 3a showed a singlet at  $-3545.99$  ppm, which is downfield shifted compared with that of the precursor 1 ( $-4333.82$  ppm). These aforementioned experiments unambiguously indicate the in situ formation of the intermediate  $[(\text{cAAC})_2\text{Pt}(\text{O}_2)]$  (3a), which then further reacts with  $\text{S}_8$  to produce the stable and crystalline complex 4a. However, we were not able to crystallize the intermediate species 3a after several efforts. The brown crystals of 4a are stable in air for several days at room temperature. The UV/Vis spectrum of 4a was recorded in THF, which showed broad absorption bands at  $\lambda = 390$  and  $550$  nm (see the Supporting Information). Compound 4a was further characterized by mass spectrometry in MeCN ( $[\text{M}+\text{H}]^+$   $m/z$ : 918.4774; see the Supporting Information), NMR spectroscopy and X-ray single-crystal structural analysis.

Complex 2a crystallizes in the monoclinic space group  $\text{C2}/c$  with a lattice solvent molecule (THF) within the asymmetric unit. The molecular structure of 2a is displayed in Figure 1 (top), which shows the formation of a three-membered  $\text{PtS}_2$  ring, in which the central platinum atom adopts a distorted square planar geometry with a C–Pt–C bond angle of  $109.9(2)^\circ$ , which is smaller compared with that of the precursor 1a  $(\text{cAAC})_2\text{Pt}$  ( $169.53(6)^\circ$ )<sup>[14]</sup> and coordinated with two carbene ( $\text{Et}_2\text{-cAAC}$ ) rings. The  $\text{C}_{\text{carbene}}\text{-Pt}$  distances of 2a ( $2.003(2)$  Å) are slightly longer when compared with those of 1a (ca.  $1.97$  Å).<sup>[14]</sup> The  $\text{C}_{\text{carbene}}\text{-N}$  bond distance in 2 ( $1.329(2)$  Å) is very close to that of 1a (ca.  $1.326$  Å).<sup>[14]</sup> Two five-membered carbene rings are oriented in *trans* conformation with respect to the  $\text{PtS}_2$  three-membered ring. The Pt–S/S–S bond lengths in 2a are  $2.356(1)$  and  $2.067(2)$  Å, respectively.

Complex 4a crystallizes in the monoclinic space group  $\text{P2}_1/c$ . The molecular structure of 4a is depicted in Figure 1 (bottom), in which a four-membered  $\text{PtO}_2\text{S}$  ring is formed by the side-on coordination of the sulfate anion, disordered with the  $\text{PtS}_2$  ring of the starting material in a 1:1 ratio. The central platinum atom adopts a near tetrahedral geometry with a C–Pt–C bond angle of  $107.4(2)^\circ$ , which is slightly smaller than that of 2a. The two carbene rings are oriented in *trans* conformation with respect to the  $\text{S}_2/\text{PtSO}_4$  unit. The Pt–S bond lengths in 4a are in the range of  $2.371(3)$ – $2.373(3)$  Å, which are slightly longer compared to 2a. The small difference in the  $\text{PtS}_2$  bond lengths can result from the disordered structure. The Pt–O distance is  $2.083(7)$ – $2.084(8)$  Å. The  $\text{C}_{\text{carbene}}\text{-Pt}$  distances of 4a ( $1.997(3)$ –

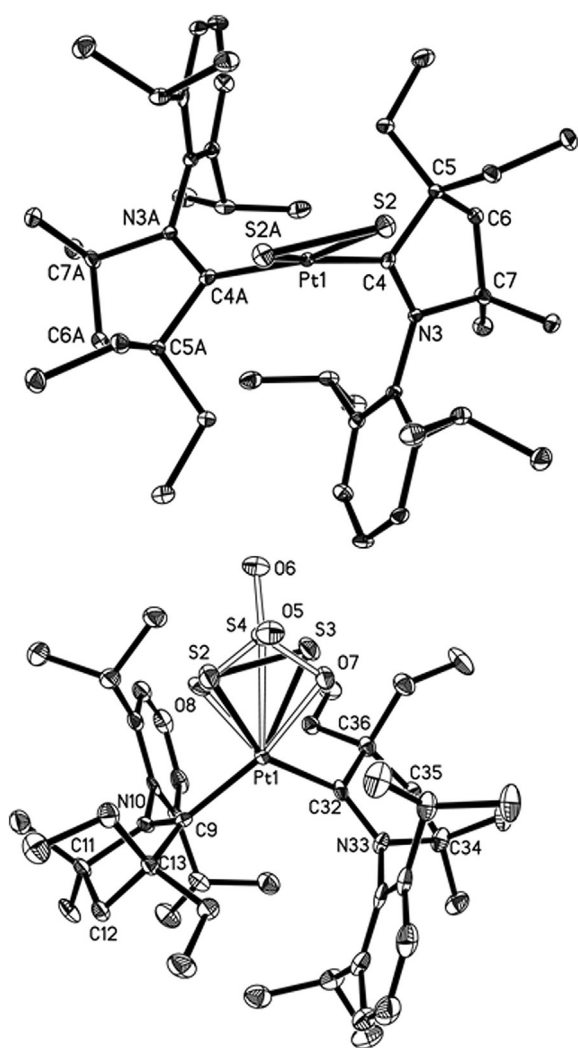


**Figure 1.** Molecular structures of complexes **2a** (top) and **4a** (bottom). Hydrogen atoms are omitted for clarity. Selected experimental (calculated at R-M06/def2-SVP for the singlet state) bond lengths [Å] and angles [°] for **2a**: Pt1–C4 2.003(2) [2.037], Pt1–S2 2.356(1) [2.410], S2–S2' 2.067(2) [2.083], C4–N3 1.329(2) [1.337]; C4–N3–C7 114.1(2) [113.7], C4–Pt1–C4' 109.9(2) [112.2], S2–Pt1–S2' 52.02(3) [51.2], S2–S2'–Pt1 63.99(2) [64.4]. For **4a**: 1:1 S<sub>2</sub>/SO<sub>4</sub> disorder, Pt1–C9 2.003(3) [2.004], Pt1–C32 1.997(3) [2.004], Pt1–S2 2.373(3), Pt1–S3 2.371(3), S2–S3 2.067(4), Pt1–O7 2.083(7) [2.099], Pt1–O8 2.084(8) [2.099], S4–O5 1.439(5) [1.456], S4–O6 1.440(5) [1.456], S4–O7 1.555(6) [1.584], S4–O8 1.548(7) [1.584], C9–N10 1.325(4) [1.329]; C9–N10–C11 114.2(3) [114.1], C9–Pt1–C32 107.4(2) [106.0].

2.003(3) Å) are the same compared with those of **2a**. The C<sub>carbene</sub>–N bond length in **4a** is about the same (1.325(4) Å) as that of **2a**. The S–O distances of the platinum-coordinated oxygen atoms are on average 0.12 Å longer than those of the pendent oxygen atoms O5 and O6, emphasizing the partly ionic S–O bond character.<sup>[15]</sup>

To explore the electronic structure and bonding environment, geometry optimization of **2a**, **3a**, and **4a** were accomplished at the M06/def2-SVP level of theory (for computational details, see the Supporting Information). The computed bond lengths and bond angles of **2a** and **4a** showed good agreement with the experimentally obtained geometrical parameters, as can be seen from alignments and superposition plot

(Figure S7 and Table S1 in the Supporting Information). The natural bond orbital (NBO) population analysis of **2a** entails that the Pt1 atom is connected with S2/S2' and C4/C4' through single-bond occupancies of 1.870 and 1.889 e, respectively (Table S2 in the Supporting Information). The C4/C4' atoms have main contribution towards electron density (ca. 72.3%) in the Pt1–C4/Pt1–C4' bonds. Similarly, S2/S2' atoms donate approximately 67.3% to form Pt1–S2/Pt1–S2' bonds in both cases, indicating a polar character. This result is supported by the properties of the bond-critical point (BCP) elucidated from quantum theory of atoms in molecules (QTAIM) calculations.<sup>[16]</sup> The important topological parameters at the (3,-1) bond critical points are given in Table S3. The electron density [ $\rho(r)$ ] at the BCP of Pt1–C4/Pt1–C4' [0.138] and Pt1–S2/Pt1–S2' [0.086] bonds along with the respective Laplacian [ $\nabla^2\rho(r)$ ; +0.233, and +0.129] indicates significant donor–acceptor-type interaction. The NPA charge on Pt1 ( $q_{\text{Pt1}}=0.030$ ) in **2a** is higher than the precursor complex **1a** ( $q_{\text{Pt1}}=-0.350$ ), reflecting electron depletion from the Pt1 to the sulfur atom. The amount of charge transfer is collected in Tables S4 and S5 in the Supporting Information. This result can also be perceived by visualizing the frontier orbital of **2a** and **1a**. After electron depletion, the HOMO of **2a** showed d<sub>xy</sub> orbital character at the Pt1 atom similar to HOMO–1 of **1a** (Figures 2 and S8 in the Supporting Information). The Wiberg bond indices of Pt1–C4/Pt1–C4' and

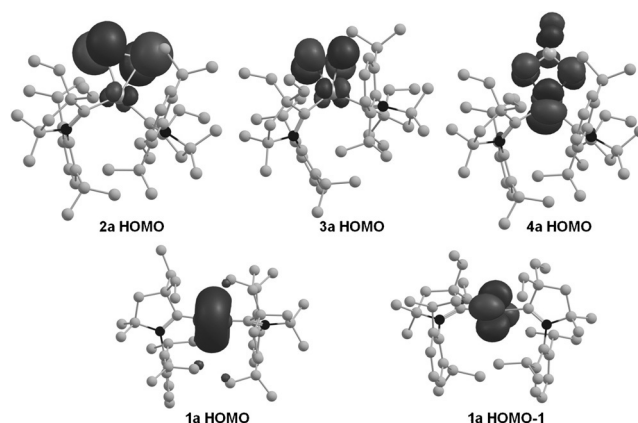


**Figure 2.** Selected KS-MOs of **2a**, **3a**, **4a**, and **1a** (isosurface 0.04 a.u.). Hydrogen atoms are omitted for clarity.

Pt1–S2/Pt1–S2' bonds were calculated to be 0.67 and 0.62, respectively. The calculated Pt–C<sub>carbene</sub> distance in **2a** is relatively longer than that of the precursor **1**, this signifies less back donation from Pt1 to the C<sub>carbene</sub> (2.037 Å in **2a** vs. 2.019 Å in **1**). It is also evident from the NPA charge at the C<sub>carbene</sub> atom (0.290 in **2a** vs. 0.198 in **1a**) and the Wiberg index of the Pt–C<sub>carbene</sub> bond (0.67 in **2a** vs. 0.73 in **1a**). The application of the second-order perturbation theory within the NBO analysis revealed that the occurrence of the stabilizing two-electron donor–acceptor interaction from the lone pair of Pt1 [LP(Pt1)] to the empty orbital [LP\*(S2)] of the S2 atom and from the S2 lone pair [LP(S2)] to the anti-bonding orbital of Pt–C<sub>carbene</sub> bond. The computed associated energies are 66.8 and 106.4 kcal

mol<sup>-1</sup> for [LP(Pt1)]→[LP\*(S2)] and [LP(S2)]→σ\*(Pt–C<sub>carbene</sub>), respectively. Similar to **2a**, C9/C32 (ca. 69.9%) atoms in **4a** have main contribution towards the formation of Pt1–C9/Pt1–C32 bonds having single-bond occupancies of 1.891 e. The symmetrical nature of the structure showed identical (Pt1–O7/Pt1–O8 = 2.099 Å) bond lengths. The AIM (Atoms in Molecules) parameter clearly suggested closed-shell-type interaction to be present in the Pt1–O7/Pt1–O8 bond ( $\rho(r)/\nabla^2\rho(r) = 0.099/0.363$ , Table S3 in the Supporting Information). The charge on Pt1 ( $q_{\text{Pt1}} = 0.471$  e) is much more depleted, and  $\chi_{\text{C}_{\text{carbene}}-\text{Pt}-\text{C}_{\text{carbene}}}$  largely deviates from **1a** ( $\chi_{\text{C}_{\text{carbene}}-\text{Pt}-\text{C}_{\text{carbene}}} = 112.2$  in **2a** vs. 170.7 in **1a**). In a similar vein, the bonding scenario of the transient intermediate **3a** was further investigated at the same level of theory. Similar to **2a**, Pt1–C4/Pt1–C4' bond showed donor–acceptor [ $\rho(r)/\nabla^2\rho(r) = 0.145/0.241$ ] type interactions (Table S3 in the Supporting Information). A greater polar character of Pt1–O1/Pt1–O2 bonds in **3a** than Pt1–S2/Pt1–S2' bonds in **2a** [ $\rho(r)/\nabla^2\rho(r) = 0.119/0.433$  vs. 0.086/0.128] is a direct consequence of higher electronegativity of oxygen than sulfur. Analogous to **2a**, the charge on Pt1 (0.406) is much higher, indicating superior charge transfer from Pt1 to the oxygen moiety (Tables S4 and S5 in the Supporting Information). The Wiberg bond index for Pt1–O1/Pt1–O2 (WBI 0.50) bonds are lower than the Pt1–S2/Pt1–S2' (0.62) bonds, stipulating relative weaker Pt1–O1/Pt1–O2 bonds.

To explain the UV/Vis spectra, we have performed the time-dependent (TD) DFT calculations at the M06/def2-TZVP/SMD//M06/def2-SVP level of theory under implicit THF environment. Complex **2a** exhibited the characteristic band at  $\lambda = 584.3$  nm with an oscillator strength of 0.02, designating the LP<sub>S2–S2'</sub>→ $\pi^*_{\text{C4–N3/C4'–N3'}}$ , which is in line with the experimentally observed band at  $\lambda = 575$  nm. This can be considered as intramolecular ligand-to-ligand charge transfer. It is in line with the lower lying LUMO of cAAC in **2a**.<sup>[10,11]</sup> However, complex **4a** showed signature bands at  $\lambda = 291.3$  nm and 341.5 nm, primarily due to the transition from Pt1  $d_{xy}/d_{z^2}$ → $\pi^*_{\text{C–N}}$ . The relatively higher deviation from experimentally observed bands at  $\lambda = 390$  nm and 550 nm might be due to the [S<sub>2</sub>/SO<sub>4</sub>] disorder present in the crystal of **4a** (Figures 2, S8 and Table S6 in the Supporting Information). The TDDFT analysis of **3a** gave four main excitations at 256.5 nm (HOMO–1→LUMO+2), 317.2 nm (HOMO–3→LUMO), 358.5 nm (HOMO–2→LUMO), and 401.5 nm (HOMO→LUMO+1), respectively, which are in close agreement with the experimental data (see above).

In conclusion, we have developed the syntheses protocol for the cAAC-stabilized air-stable monomeric [(cAAC)<sub>2</sub>Pt(S<sub>2</sub>)] (**2**) and the [(cAAC)<sub>2</sub>Pt(SO<sub>4</sub>)<sub>x</sub>(S<sub>2</sub>)<sub>1–x</sub>] (**4**), which were prepared by the reaction of (cAAC)<sub>2</sub>Pt (**1**) with elemental sulfur. Complex **4** was formed when **2** was exposed to air. NMR spectroscopic studies and theoretical calculations showed that complex **4** was formed via the in situ generated intermediate [(cAAC)<sub>2</sub>Pt(O<sub>2</sub>)] (**3**), which has been characterized by MS (EI) spectrometry and NMR spectroscopy. The binding of O<sub>2</sub> at the Pt<sup>0</sup> center was found to be reversible. The monomeric molecular structures of **2** and **4** have been confirmed by X-ray single-crystal diffraction analysis, and they were also characterized by NMR and UV/Vis spectroscopy. DFT calculations revealed that the formation of **2**

from the initial precursor **1** is energetically favorable by 13.1 kcal mol<sup>-1</sup>. In contrast, the in situ formation of dioxygen analogue **3** is endergonic by 12.1 kcal mol<sup>-1</sup>. The donor–acceptor-type interactions of Pt–S bonds in **2** and Pt–O bonds in **3** and **4** have been theoretically confirmed.

## Experimental Section

**Crystal data for 2a at 100(2) K:** C<sub>52</sub>H<sub>86</sub>N<sub>2</sub>O<sub>2</sub>PtS<sub>2</sub>,  $M_r = 1030.43$  g mol<sup>-1</sup>, 0.178×0.114×0.065 mm, monoclinic, C2/c,  $a = 29.646(2)$ ,  $b = 10.870(2)$ ,  $c = 18.065(3)$  Å,  $\beta = 125.02(2)^\circ$ ,  $V = 4767.5(16)$  Å<sup>3</sup>,  $Z = 4$ ,  $\mu$  (Ag<sub>K $\alpha$</sub> ) = 1.672 mm<sup>-1</sup>,  $2\theta_{\text{max}} = 22^\circ$ , 51 764 reflections measured, 5942 independent ( $R_{\text{int}} = 0.0591$ )  $R_1 = 0.0223$  [ $I > 2\sigma(I)$ ],  $wR_2 = 0.0436$  (all data), res. density peaks: 0.578 to –0.751 e Å<sup>-3</sup>.

**Crystal data for 4a at 100(2) K:** C<sub>44</sub>H<sub>70</sub>N<sub>2</sub>O<sub>1.98</sub>PtS<sub>1.50</sub>,  $M_r = 902.08$  g mol<sup>-1</sup>, 0.158×0.123×0.088 mm, monoclinic, P2<sub>1</sub>/c,  $a = 11.473(2)$ ,  $b = 20.772(3)$ ,  $c = 17.246(2)$  Å,  $\beta = 95.42(2)^\circ$ ,  $V = 4091.6(10)$  Å<sup>3</sup>,  $Z = 4$ ,  $\mu$  (Ag<sub>K $\alpha$</sub> ) = 1.929 mm<sup>-1</sup>,  $2\theta_{\text{max}} = 22^\circ$ , 121 963 reflections measured, 10 139 independent ( $R_{\text{int}} = 0.0728$ ),  $R_1 = 0.0344$  [ $I > 2\sigma(I)$ ],  $wR_2 = 0.0548$  (all data), res. density peaks: 0.899 to –1.489 e Å<sup>-3</sup>.

CCDC 1444046 and 1444047 contain the supplementary crystallographic data for this paper. These data are provided free of charge by The Cambridge Crystallographic Data Centre

All crystals were selected under cooling, using a X-Temp2 device.<sup>[17]</sup> The data were integrated with SAINT.<sup>[18]</sup> A multiscan absorption correction was applied by using SADABS.<sup>[19]</sup> The structures were solved by SHELXT<sup>[20]</sup> and refined on  $F^2$  by using SHELXL<sup>[21]</sup> in the graphical user interface SHELXL.<sup>[22]</sup>

## Acknowledgements

H.W.R. thanks the Deutsche Forschungsgemeinschaft (DFG RO 224/60-I) for financial support. D.S. thanks the Fonds der Chemischen Industrie and the Danish National Research Foundation (DNRF93) funded Centre for Materials Crystallography (CMC) for financial support. T.M. thanks CSIR for a SRF fellowship, and D.K. acknowledge IISER-Kolkata and the CSIR project fund (01(2770)/13/EMR-II) for financial support. S.R. thanks Dr. P. P. Samuel for UV/Vis plots.

**Keywords:** carbenes · density functional calculations · monomeric PtS<sub>2</sub> · platinum · sulfur

- [1] E. Davey, *J. Chem. Phys.* **1814**, 10, 382.
- [2] a) A. Kjekshus, F. Grønvold, *Acta Chem. Scand.* **1959**, 13, 1767; b) F. Grønvold, H. Haraldsen, A. Kjekshus, *Acta Chem. Scand.* **1960**, 14, 1879.
- [3] a) J. A. Wilson, A. D. Yoffe, *Adv. Phys.* **1969**, 18, 193; b) P. Miró, M. Ghorbani-Asl, T. Heine, *Angew. Chem. Int. Ed.* **2014**, 53, 3015; *Angew. Chem.* **2014**, 126, 3059.
- [4] A. Müller, B. Krebs, *Sulfur, Its Significance for Chemistry, for the Geo-, Bio-, and Cosmosphere and Technology*, Elsevier, Amsterdam, **1984**.
- [5] a) K. Isobe, Y. Ozawa, A. Vázquez de Miguel, T.-W. Zhu, K.-M. Zhao, T. Nishioka, T. Ogura, T. Kitagawa, *Angew. Chem. Int. Ed. Engl.* **1994**, 33, 1882; *Angew. Chem.* **1994**, 106, 1934; b) K. Shiomi, B. K. Breedlove, H. Kitayama, T. Nishioka, I. Kinoshita, N. Koga, K. Isobe, *Chem. Commun.* **2002**, 1756; c) D. Stalke, *Chem. Commun.* **2012**, 48, 9559.
- [6] a) T. Nishioka, H. Kitayama, B. K. Breedlove, K. Shiomi, I. Kinoshita, K. Isobe, *Inorg. Chem.* **2004**, 43, 5688; b) T. S. Lobana, K. Isobe, H. Kitayama, T. Nishioka, I. Kinoshita, *Angew. Chem. Int. Ed.* **2004**, 43, 213; *Angew.*

- Chem.* **2004**, *116*, 215; c) T. S. Lobana, K. Isobe, H. Kitayama, T. Nishioka, M. Doe, I. Kinoshita, *Organometallics* **2004**, *23*, 5347.
- [7] a) A. Ishii, M. Murata, H. Oshida, K. Matsumoto, J. Nakayama, *Eur. J. Inorg. Chem.* **2003**, 3716; b) T. Saito, T. Sunaga, N. Sakai, Y. Nakamura, S. Yamamoto, D. Iriuchijima, K. Yoza, *Inorg. Chem.* **2005**, *44*, 4427; c) A. Z. Rys, A.-M. Lebuis, A. Shaver, *Inorg. Chem.* **2006**, *45*, 341; d) K. Oya, H. Seino, M. Akiizumi, Y. Mizobe, *Organometallics* **2011**, *30*, 2939; e) H. S. Yu, D. G. Truhlar, *Angew. Chem. Int. Ed.* **2016**, DOI: 10.1002/anie.201604670.
- [8] a) S. L. Chatwin, R. A. Diggle, R. F. R. Jazzar, S. A. Macgregor, M. F. Mahon, M. K. Whittlesey, *Inorg. Chem.* **2003**, *42*, 7695; b) A. Müller, W. Jaegermann, *Inorg. Chem.* **1979**, *18*, 2631; c) C. M. Bolinger, T. B. Rauchfuss, A. L. Rheingold, *Organometallics* **1982**, *1*, 1551; d) P. M. Boorman, K. A. Kerr, R. A. Kydd, K. J. Moynihan, K. A. Valentine, *J. Chem. Soc. Dalton Trans.* **1982**, 1401; e) C. M. Bolinger, T. B. Rauchfuss, A. L. Rheingold, *J. Am. Chem. Soc.* **1983**, *105*, 6321; f) C. A. McConnachie, E. I. Stiefel, *Inorg. Chem.* **1999**, *38*, 964; g) L. Y. Goh, T. C. W. Mak, *J. Chem. Soc. Chem. Commun.* **1986**, 1474; h) J. Wachter, *Angew. Chem. Int. Ed. Engl.* **1989**, *28*, 1613; *Angew. Chem.* **1989**, *101*, 1645 and references therein; i) A. Müller, W. Jaegermann, J. H. Enemark, *Coord. Chem. Rev.* **1982**, *46*, 245.
- [9] a) J. Li, F. Li, L. L. Koh, T. S. A. Hor, *Dalton Trans.* **2010**, *39*, 2441; b) Y. Maeda, H. Hashimoto, T. Nishioka, *Dalton Trans.* **2012**, *41*, 12038.
- [10] V. Lavallo, Y. Canac, C. Präsang, B. Donnadieu, G. Bertrand, *Angew. Chem. Int. Ed.* **2005**, *44*, 5705; *Angew. Chem.* **2005**, *117*, 5851.
- [11] a) D. Martin, M. Soleilhavoup, G. Bertrand, *Chem. Sci.* **2011**, *2*, 389; b) K. C. Mondal, H. W. Roesky, M. C. Schwarzer, G. Frenking, B. Niepötter, H. Wolf, R. Herbst-Irmer, D. Stalke, *Angew. Chem. Int. Ed.* **2013**, *52*, 2963; *Angew. Chem.* **2013**, *125*, 3036; *Angew. Chem. Angew. Chem.* **2013**, *125*, 3036; c) B. Niepötter, R. Herbst-Irmer, D. Kratzert, P. P. Samuel, K. C. Mondal, H. W. Roesky, P. Jerabek, G. Frenking, D. Stalke, *Angew. Chem. Int. Ed.* **2014**, *53*, 2766; *Angew. Chem.* **2014**, *126*, 2806.
- [12] a) K. C. Mondal, P. P. Samuel, Y. Li, S. Roy, H. W. Roesky, L. Ackermann, N. S. Sidhu, G. M. Sheldrick, C. Carl, S. Demeshko, S. De, P. Parameswaran, L. Ungur, L. F. Chibotaru, D. M. Andrada, *Eur. J. Inorg. Chem.* **2014**, 818; b) S. Roy, K. C. Mondal, J. Meyer, B. Niepötter, C. Köhler, R. Herbst-Irmer, D. Stalke, B. Dittrich, D. M. Andrada, G. Frenking, H. W. Roesky, *Chem. Eur. J.* **2015**, *21*, 9312.
- [13] a) P. P. Samuel, K. C. Mondal, H. W. Roesky, M. Hermann, G. Frenking, S. Demeshko, F. Meyer, A. C. Stückl, J. H. Christian, N. S. Dalal, L. Ungur, L. F. Chibotaru, K. Pröpper, A. Meents, B. Dittrich, *Angew. Chem. Int. Ed.* **2013**, *52*, 11817; *Angew. Chem.* **2013**, *125*, 12033; b) P. M. Treichel, G. P. Werber, *J. Am. Chem. Soc.* **1968**, *90*, 1753; c) W. D. Bonds Jr., J. A. Ibers, *J. Am. Chem. Soc.* **1972**, *94*, 3413; d) A. P. Ginsberg, W. E. Lindsell, *Chem. Commun.* **1971**, 232; e) G. Schmid, G. Ritter, T. Debaerdemaeker, *Chem. Ber.* **1975**, *108*, 3008; f) G. Schmid, G. Ritter, *Angew. Chem. Int. Ed. Engl.* **1975**, *14*, 645; *Angew. Chem.* **1975**, *87*, 673; g) J. E. Hoots, D. A. Lesch, T. B. Rauchfuss, *Inorg. Chem.* **1984**, *23*, 3130.
- [14] Ref. [12].
- [15] M. S. Schmökel, S. Cenedese, J. Overgaard, M. R. V. Jørgensen, Y.-S. Chen, C. Gatti, D. Stalke, B. B. Iversen, *Inorg. Chem.* **2012**, *51*, 8607.
- [16] R. F. W. Bader, *Atoms in Molecules: A Quantum Theory*, Clarendon Press, Oxford, **1990**.
- [17] a) D. Stalke, *Chem. Soc. Rev.* **1998**, *27*, 171; b) T. Kottke, D. Stalke, *J. Appl. Crystallogr.* **1993**, *26*, 615.
- [18] Bruker AXS Inc., in *Bruker Apex CCD, SAINT v8.30C*, Bruker AXS Inst. Inc., WI, Madison, **2013**.
- [19] L. Krause, R. Herbst-Irmer, G. M. Sheldrick, D. Stalke, *J. Appl. Crystallogr.* **2015**, *48*, 3.
- [20] G. M. Sheldrick, *Acta Crystallogr. A* **2015**, *71*, 3.
- [21] G. M. Sheldrick, *Acta Crystallogr. C* **2015**, *71*, 3.
- [22] C. B. Hübschle, G. M. Sheldrick, B. Dittrich, *J. Appl. Crystallogr.* **2011**, *44*, 1281.

---

Received: June 25, 2016